J Nanostruct 12(3): 607-615, Summer 2022

RESEARCH PAPER

Fabrication of Iron-Cobalt-Indium Alloy Nanowires in AAO Template by AC Electrodeposition: Investigation of the Indium Concentrations on the Magnetic Properties of Nanowires

*Sahar Mottaghian [1], Mojgan Najafi [2] *, Amir Abbas Rafati [3], Seyed Ali AsgharTerohid [1]*

[1] *Department of Physics, Hamedan Branch, Islamic Azad University, Hamedan, Iran*

[2] *Department of Materials Engineering, Hamedan University of Technology (HUT), Hamedan, Iran*

[3] *Department of Physical Chemistry, Faculty of Chemistry, Bu-Ali Sina University, Hamedan, Iran*

ARTICLE INFO

Article History:
Received 18 February 2022
Accepted 09 June 2022
Published 01 July 2022

Keywords:
Anodic aluminum oxide (AAO)
Cobalt-iron-indium alloy
Electrodeposition
Magnetic properties
Nanowires;

ABSTRACT

Iron-cobalt and iron-cobalt-indium nanowires were fabricated with a diameter of 32 nm. Iron-cobalt and iron-cobalt-indium alloy nanowire arrays were grown using AC electrodeposition into nanopores of anodic aluminum oxide (AAO) template. Anodic aluminum oxide template with a diameter of 32 nm and a distance between holes of 100 nm was synthesized as a template by using the two-step anodizing method of aluminum foil and using oxalic acid. The effect of adding indium impurities on the magnetic properties of iron-cobalt nanowires was studied. Indium impurities with different amounts were added to iron-cobalt nanowires by varying the concentrations of indium ions in the electrocoagulation solution. The results showed that the coercivity of iron-cobalt nanowires was reduced by adding indium impurity as a nonmagnetic material from 1854 Oe to 801 Oe by adding 0.05M In-ions in the electrochemical bath during electrodeposition. The crystalline structure of the nanowires was concentration dependent and change of bcc structure of CoFe to amorphous and then cubic structure of Indium. The broadening of the spectrum along the Hc axis of FORC analysis shows that the magnetization reversal in the domains of nanowires is diverse and the interaction between of the adjacent nanowires in the template is low.

How to cite this article
Dehghankelishadi P, Dorkoosh FA. Fabrication of Iron-Cobalt-Indium Alloy Nanowires in AAO Template by AC Electrodeposition: Investigation of the Indium Concentrations on the Magnetic Properties of Nanowires
J Nanostruct, 2022; 12(3):607-615. DOI: 10.22052/JNS.2022.03.014

INTRODUCTION

Arrays of one-dimensional nanostructured materials such as magnetic nanowires have attracted a great deal of attention not only for fundamental physical interest but also practical applications, such as high-density perpendicular magnetic recording medium, sensors, biosensors, supercapacitors, electromagnetic devices [1-3]. Template-assisted method for fabricating of magnetic nanowires inside the nanopores of highly hexagonally ordered porous anodic aluminum oxide (AAO), through electrochemical deposition technique has been widely studied over the last decades [4-6]. This process has been established as a low cost and high-efficiency fabrication procedure of nanowire arrays with controlled geometrical parameters (the length, diameter and density of nanowires). Also, the properties of nanowires can be controlled by the electrolyte composition and pH, electrodeposition frequency, voltage and current [7-9]. In the past few decades, extensive research has been carried out on

* *Corresponding Author Email: mojgannajafi1@gmail.com*

binary and ternary ferromagnetic alloy nanowires for their tunable magnetism with variations in elemental proportions. FeCo nanowire arrays are very interested because of their relatively low crystallization energy, high saturation magnetization (Ms), elevated Curie temperature as well as large magnetic anisotropy that make them suitable for several applications ranging from spintronics to biomedical applications [10]. The magnetic properties of FeCo alloy can be tuned and enhanced with the substitution of other elements or changing the composition ratio. To improve the magnetic properties of FeCo magnetic nanowires, the substitution of different elements such as B, P, Cu, Zn, Ni, and Pb. were investigated [11-16]. However, no report has been published regarding indium in CoFe alloy nanowires. In this paper, for the first time we show results on the synthesis of CoFeIn nanowires with the different percentages of elements· Our results show that magnetic properties and crystalline microstructures and morphology of CoFe nanowire changed by the different percentages of indium in CoFe nanowires.

MATERIALS AND METHODS

The chemicals and reagents used were of analytical grade (Merck) and used without further purification. All aqueous solutions were prepared using double distilled water at room temperature. Porous aluminum oxide templates were prepared using 0.3 mm thick aluminum sheets with high purity (99.99%) by the two-step anodizing method. By using high purity aluminum foil, reduce internal stress during anodizing, which leads to the formation of a high order structure alumina structure. Then punched circle samples by 8mm diameter degreased with acetone for 6 minutes in an ultrasonic device and then annealed for 20 minutes at 450 ° C in Ar atmosphere. To remove the oxide layer on the aluminum surface, the samples were immersed in 3M solution of caustic soda for 4 minutes. Before anodizing, the samples were electropolished in a 1:4 (vol/vol) mixture of perchloric acid ($HClO_4$) and ethanol C_2H_5OH by applying a constant voltage of 25 V for 6 min to reduce the surface microscopic roughness and obtained mirror-like surface. Then, the anodizing processes of the sample was performed in two steps: The first step was done in a two-electrode cell consisting of the sample as the anode electrode and platinum electrode as the cathode electrode with a solution of 0.3 M oxalic acid as the electrolyte. It was performed under voltage of 40V for 24 hours at 7°C. Before performing the second anodizing step, the aluminum oxide layer formed in the first step must be removed. For this purpose, the anodized samples were immersed in 0.3 M chromium trioxide and 0.5 M phosphoric acid for 24 hours at 40 ° C. The second anodizing step was similar to the first step, except that the duration of this step is 1 hour. During the anodizing process, a non-conductive layer of alumina (barrier layer) is formed between the end of the conductive aluminum and the cavities. When using the template as an electrode in the electrodeposition process, this non-conductive layer prevents electron transfer. Therefore, to facilitate the electron transfer process, this barrier layer should be as thin as possible. The thinning process of the barrier layer was done in 3 steps from 40 to 8 volts. At first, the voltage decreased by 4V/min from 40V to 20V, then to 10 V by 2 V/min and finally to 8 volts by 1V/min. At the end of the third stage, anodizing was continued for 3 minutes at 8 V to obtain a uniform and homogeneous thin barrier layer [25]. In this work, the synthesis and characterization of CoFeIn nanowire arrays with different compositions fabricated by AC electrodeposition in nanoporous alumina templates are reported. The electrolytic bath contains $CoSO_4.7H_2O$, $Fe_2SO_4.7H_2O$, $InCl_3$, and boric acid and ascorbic acid. Boric acid is used to keep the pH constant and ascorbic acid is used to prevent the conversion of Fe^{+2} to Fe^{+3}. For the generation of different percentages of indium in nanowires, the electrolyte solution contains different molar concentrations of indium chloride. The platinum plate and the template were used as the two electrodes. AC electrodeposition was performed by Sinewave at a frequency of 200 Hz and a peak-to-peak voltage of 30V at room temperature for 15 minutes. The crystallographic study of nanowires embedded in AAO was performed using the X-ray diffractometer (XRD) with CuKa (k = 1.5406 A °). The topology and composition of nanowires were characterized by scanning electron microscopy (SEM) and EDX analyzer. The Room temperature magnetic properties of alloy CoFeIn nanowires were measured in a vibrating sample magnetometer (VSM), with magnetic fields up to 2 T. The magnetic characterization of was performed by using not only hysteresis loop measurements, but also the first order reversal curve (FORC) diagram method by applying the magnetic field

parallel to the nanowire axis

RESULTS AND DISCUSSION

Fig. 1 shows the anodization current and voltage during the second anodization. After the second anodization process, the barrier layer, which exists at the interface between the metal and the porous alumina layer, is thinned by decreasing the anodization voltage steply as shown in the figure (down to 8V). This leads to the formation of a dendritic-like structure at the bottom of the pores, that improves the electrical conductivity in the sample and, therefore, the homogeneity of the subsequent electrodeposition process of the metallic nanowires.

Fig. 2-A shows the SEM image of the surface of the AAO template. The average diameter of the holes and the distance between the holes

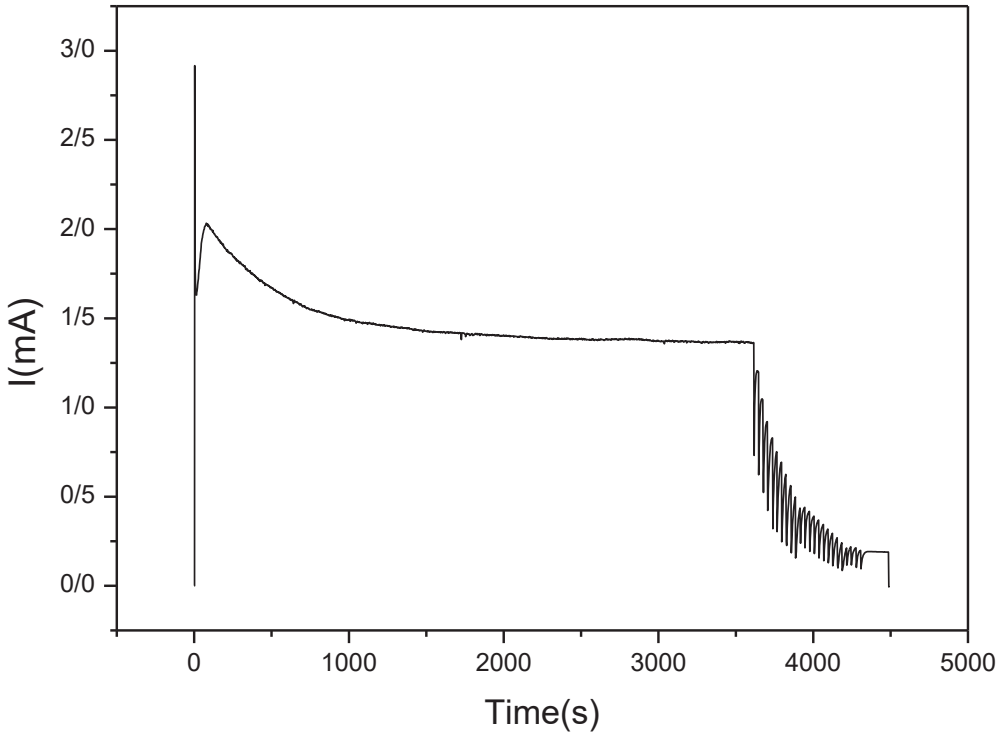

Fig. 1. The anodization current and voltage during the second anodization and barrier layer thinning process.

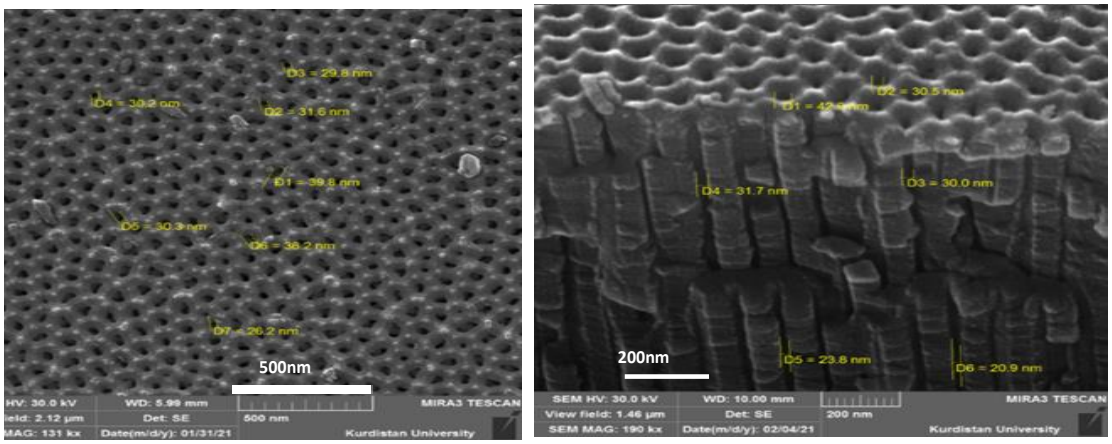

Fig. 2. The SEM image of (a) top-view the AAO template (b) the porous AAO template with the cross-sectional view of pores filled with CoFeIn NWs at 30 VPP, 200 Hz, sinusoidal waveform.

Table 1. Composition of indium, cobalt and iron electrodeposited in nanowires obtained from EDX results in terms of salt concentration of cobalt, iron and indium ions in electrodeposition solution

Concentration of ions in electrolyte solution (M)			Percentage by weight of atoms in nanowires (W%)			Sample No.
Fe^{+2}	Co^{+2}	In^{+3}	Fe	Co	In	
0.05	0.12	0	38.28	61.72	0	1
0.05	0.12	0.003	37.3	56.94	5.69	2
0.05	0.12	0.006	31.28	52.17	16.55	3
0.05	0.12	0.012	25.51	47.84	26.65	4
0.05	0.12	0.025	21.35	38.05	40.6	5
0.05	0.12	0.05	2.99	7.38	89	6

are 32 nm and 100 nm, respectively. Fig. 2- B shows the cross-section SEM image of the nanowires in the template. The diameter of the nanowires is equal to the diameter of the holes. The nanowires are placed in parallel with a high percentage of the filling templates. To investigate the effect of indium, non-magnetic impurities, on iron cobalt nanowires, six samples with different concentrations of metal salts were made (Table 1). Percentage of reduced metals in nanowires according to different molar percentages of metal salts in electrodeposition solution was obtained from nanowires by EDX analysis. The EDX spectrum of three samples, $CoFeIn_{0.01x}$ (x=0, 1.2, 5) in Fig. 3, present the metal peaks Co, Fe & In, and the results of this analysis are summarized in Table 1

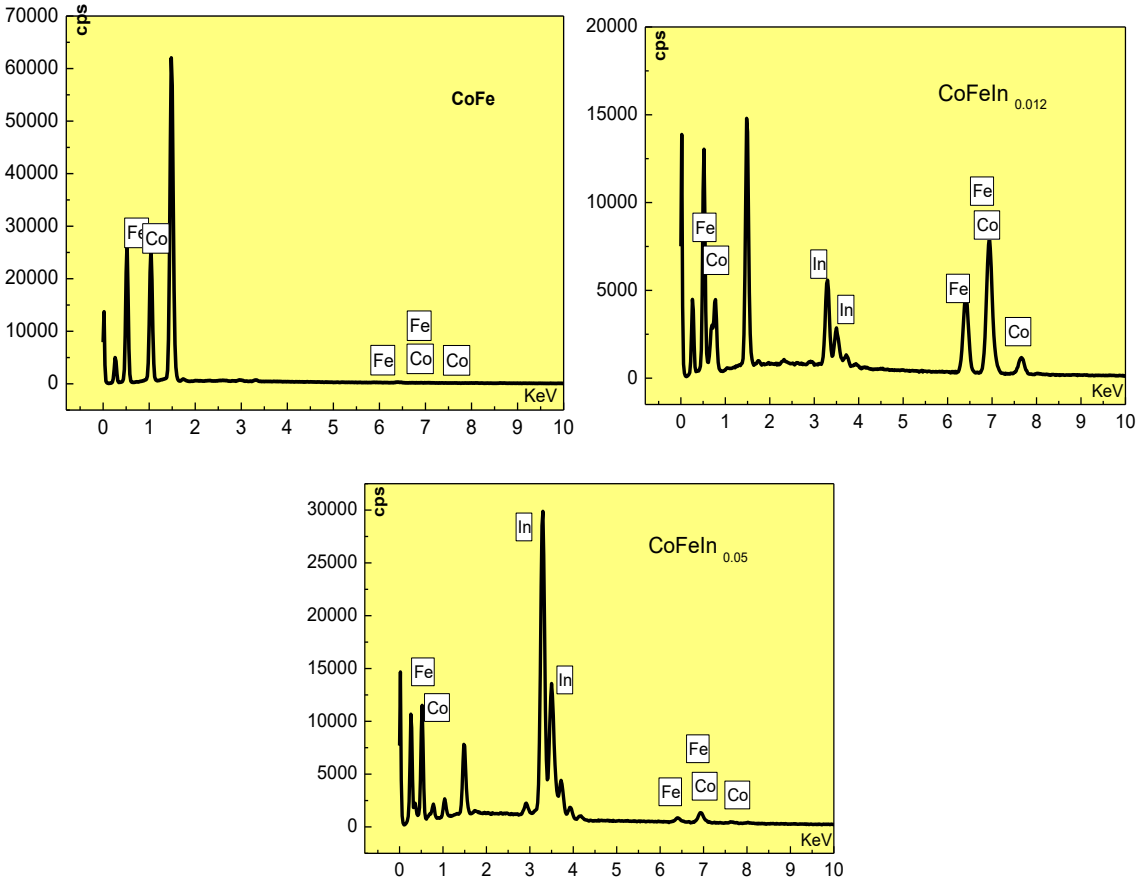

Fig. 3. The EDX patterns of $CoFeIn_{0.01x}$ (x=0, 1.2, 5) nanowires

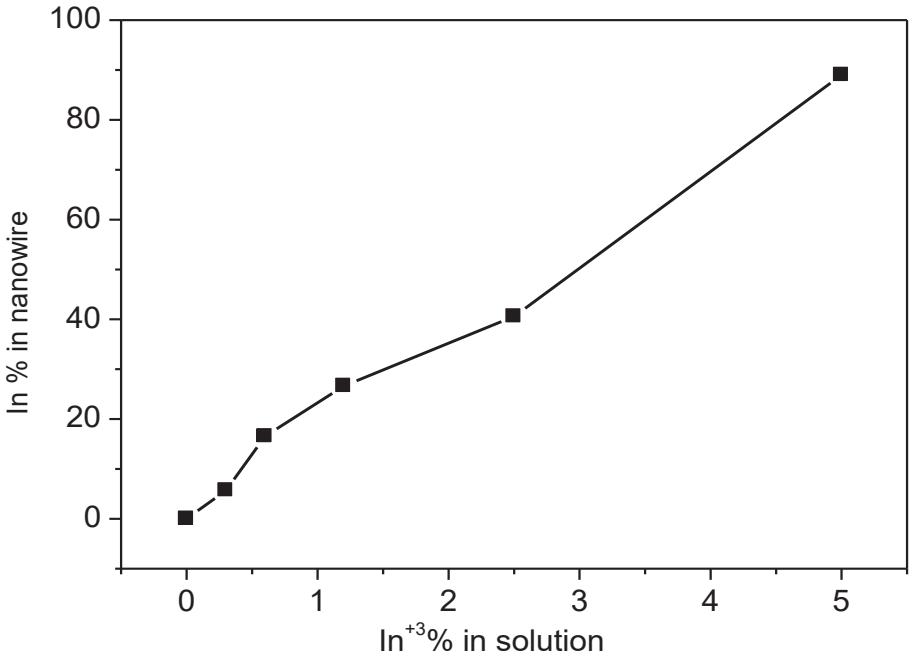

Fig. 4. Percentage of electrodeposited indium in nanowires (EDX analysis) in terms of indium salt concentration in electrolyte $CoFeIn_{0.01x}$ (x=0, 0.3, 0.6, 1.2, 2.5, 5)

and plotted in Fig. 4.

The hysteresis loops were measured by the applied external magnetic field along the nanowire axis for $CoFeIn_{0.01x}$ (x=0, 0.3, 0.6, 1.2, 2.5, 5) as shown in Fig. 5. All the loops have an almost square shape. By applying a magnetic field parallel to the axis of the nanowires (about1000 Oe), the domains rapidly align with the field, and the nanowires reach saturation magnetization. Also, by removing the external field, a significant

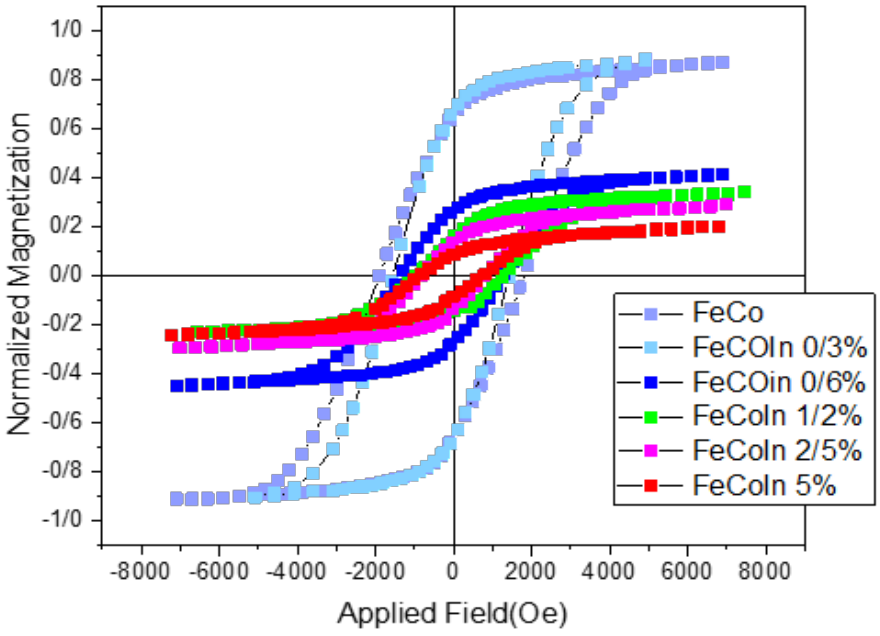

Fig. 5. Magnetic hysteresis loops of $CoFeIn_{0.01x}$ (x=0, 0.3, 0.6, 1.2, 2.5, 5) nanowires for the case of external magnetic field parallel to the nanowires.

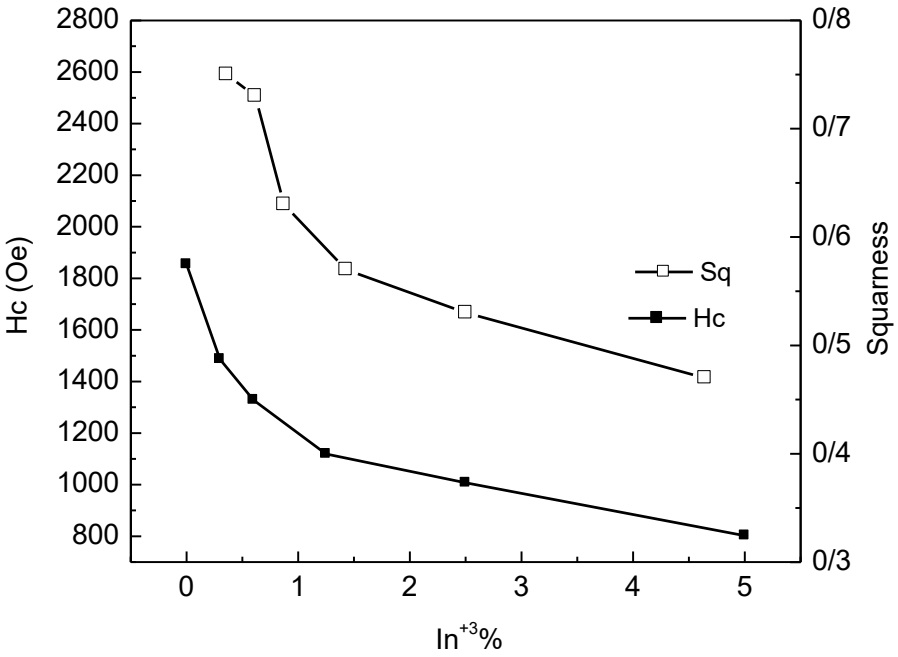

Fig. 6. Coercivity and squareness ratio dependence of the CoFeIn nanowires as a function of In content

residual magnetism remains in the nanowires. This shows that the magnetization axis easy is along the axis of the nanowires. In the other words, such a feature means that shape anisotropy is the most relevant influence in this case. The area of the loops has become smaller with the addition of indium to the nanowires. The shrinkage of the loop area is due to the increase in the amount of indium in the nanowires and the consequent increase in the atomic ratio of indium to the atomic ratio

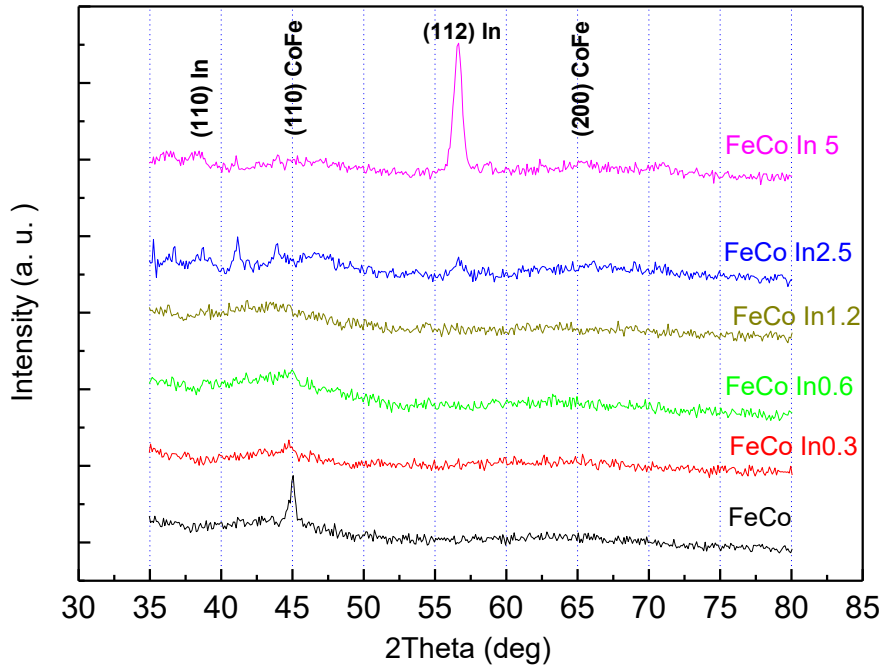

Fig. 7. XRD patterns of the $CoFeIn_{0.01x}$ (x=0, 0.3, 0.6, 1.2, 2.5, 5) nanowires as a function of indium content

of iron and cobalt in the nanowire arrays, which reduces the magnetostatic energy by decreasing the saturation magnetization. Fig. 6 displays the dependence of coercivity H_c, and squareness ratio (M_r/M_s) as a function of the different compositions of CoFeIn nanowires. The results show that the coercivity and squareness ratio of iron-cobalt nanowires is 1854 Oe and 0.74, although those are reduced to 801 Oe and 0.47 in $CoFeIn_{0.05}$. This decreasing behavior of coercivity and squareness ratio against the indium concentration is due to the addition of nonmagnetic Element (indium) and reduction of magnetic Elements (Co, Fe) and reduce the saturation magnetization M_s of samples by indium Concentration. Decreased magnetic properties along the nanowires with increasing nonmagnetic impurities have been reported. [18-19]

Fig. 7 illustrates the XRD spectra of the $CoFeIn_{0.01x}$ (in which x ranges from 0 to 5) arrays taken while they are embedded in AAO templates. For the CoFe (Sample No.1), one diffraction peak at 45.05 º with (110) plane appears in the XRD pattern, indicating this sample has bcc (body centered cubic) structure (Pm-3m) of CoFe with the c axis parallel to the NWs. With the increase of indium in samples No. 2 and 3, this CoFe peak is weak, and the structure moves towards an amorphous crystal structure, so that sample No. 4 is entirely amorphous without any peak. In sample $CoFeIn_{0.025}$ (sample No.5), two weak peaks at 2θ= 56.65 º and 36.48 º appear, and in $CoFeIn_{0.05}$ (Sample No.6), the intensity of main peak at 56.65 º degree peaks Increased Clearly. The diffraction peaks at 36.48 ºand 56.65 º with (110) and (112) planes, respectively, referred that the NWs were crystallized into the cubic structure (Fm-3m) of indium. From a crystallographic point of view, it can be said that in these six samples, first the structure of iron cobalt was seen, then with the increase of indium in the nanowire, the amorphous structure and the samples with a high percentage of indium, the crystal structure of indium appeared. The magnetization and magnetic anisotropy of nanowires is determined by the balance between shape, magnetocrystalline and magnetoelastic anisotropy terms. The contribution of magnetocrystalline anisotropy in the magnetic properties of these alloy nanowires is negligible due to their cubic phase or amorphous structure. The magnetoelastic anisotropy cannot play a relevant role in CoFe nanowires. Therefore, the magnetic properties of these nanowires are determined based on the anisotropy of the shape. The relation between magnetization in magnetostatic energy, originated by the shape anisotropy, is given as, $1/2\mu_0 N_d M^2$, N_d is the longitudinal demagnetizing factor. In samples with a higher percentage of magnetic material, the magnetization and magnetostatic energy is higher and, thus coercivity and squareness ratio along the nanowires increases. Since the distance between nanowires is the same in all samples, the role of nanowire interaction is the same in all samples.

To investigate the magnetization process of the nanowire, FORC analysis was performed by applying a field in the direction of the nanowire for the $CoFeIn_{0.6\%}$ sample, which can be seen in Fig. 8. The FORC distribution function ρ(H, H_r), which is derived from the second derivative of magnetization M (Eq. 1):

$$\rho = -\frac{1}{2}\frac{\partial^2 M(H,\ H_r)}{\partial H \partial H_r} \quad (1)$$

where H and H_r are the applied field and the reversal field, respectively. Each FORC consists of a minor loop going from a reversal field (H_r) to the saturation field. The result is represented as a contour plot ranging from blue to red and usually analyzed by employing the interaction field axis (Eq. 2) and the coercivity field axis (Eq. 3) in Preisach plane.

$$H_u = -\frac{(H + H_r)}{2} \quad (2)$$

$$H_c = \frac{(H - H_r)}{2} \quad (3)$$

It gives the statistical distribution of elementary square hysteresis loops, called mathematical hysterons. Its analysis is remarkably straightforward for nanowire arrays with longitudinal easy axis, because each hysteron can be associated to one nanowire with magnetic single-domain patterned structure. FORC diagram can statistically describe the magnetization behavior of nanowires in terms of H_c and H_u. As can be seen in Fig. 8, the single broad coercivity distribution without interaction field is observed along the H_c axis, which is attributed to the several magnetization reversals processes in nanowires. The variety of magnetization modes is related to the change of crystallographic structure to amorphous or polycrystalline phase, as concluded from XRD data and the unequal

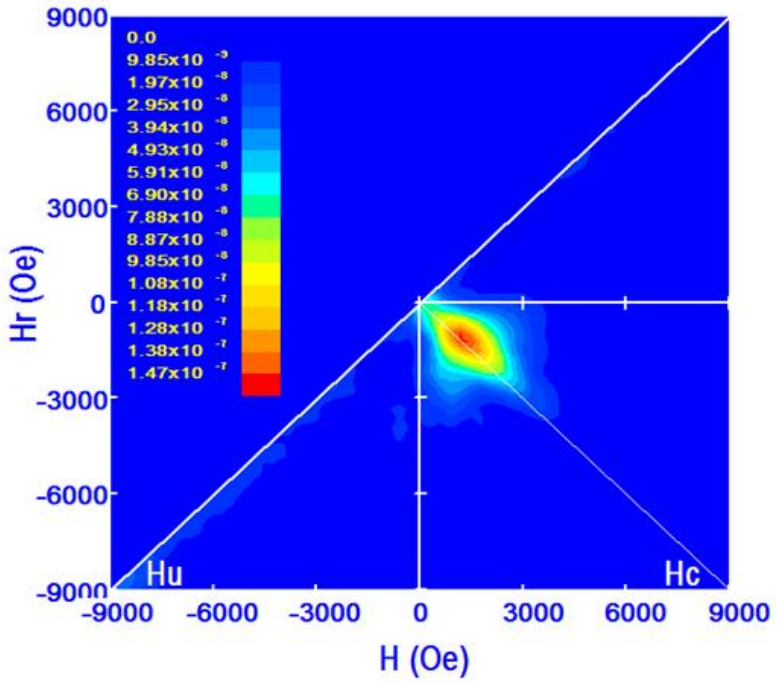

Fig. 8. FORC distribution plot of $CoFeIn_{0.006}$ nanowires in template (ΔH_r=100 Oe). The color scale goes from blue (representing the minimum) toward red (maximum values).

length of electrodeposited nanowires. In alloy nanowires, the length of the electrodeposited nanowires is not the same. The accumulation conditions along the nanowire at the beginning and end of the electrocoagulation process are not the same. The percentage of elements may be different along the nanowires. These factors cause the distribution of coercivity in nanowires. The FORC distribution along H_u is narrow, indicating that the nanowires have little interaction. For alloys in which we have a nonmagnetic material, such as indium, the distribution of FORC along the axis is low; because the nonmagnetic material reduces the magnetostatic interactions between the nanowires, this is in agreement with the EDX results, which in this sample contain 16.55% by weight of indium.

CONCLUSION

CoFeIn magnetic alloy nanowire arrays with a diameter of 32 nm and parallel to each other were made in the alumina template by AC electrodeposition method for the first time. Samples were prepared with different percentages of indium. The magnetic properties of nanowires with varying percentages of indium were measured and it was observed that as the percentage of indium increases, the coercivity decreases from 1800 Oe to 600 Oe and the squareness ratio decreases from 0.75 to 0.5, which can be explained by the presence of nonmagnetic indium in the nanowires. The structure of nanowires has changed from bcc structure of CoFe to amorphous with increasing indium in nanowires and high percentages of indium to cubic structure indium. The magnetocrystalline anisotropy for cubic and amorphous structures of these alloys has a small contribution to the magnetic properties of nanowires. FORC analysis showed that the magnetic domains in the nanowires have different magnetization reversal processes and the interaction between the nanowires is low.

CONFLICT OF INTEREST

The authors declare that there is no conflict of interests regarding the publication of this manuscript.

REFERENCES

1. Carreón-González CE, De La Torre Medina Jn, Piraux L, Encinas A. Electrodeposition Growth of Nanowire Arrays with Height Gradient Profiles for Microwave Device Applications. Nano Lett. 2011;11(5):2023-2027.
2. Jaleh B, Omidvar Dezfuli A. Pulse electrodeposition of

Ni_2Sb nanowires IN polycarbonate template. Solid State Communications. 2013;166:56-59.
3. Luo J, Cui J, Wang Y, Yu D, Qin Y, Zheng H, et al. Metal-organic framework-derived porous Cu_2O/Cu@C core-shell nanowires and their application in uric acid biosensor. Applied Surface Science. 2020;506:144662.
4. Alikhani M, Ramazani A, Almasi Kashi M, Samanifar S, Montazer AH. Irreversible evolution of angular-dependent coercivity in Fe80Ni20 nanowire arrays: Detection of a single vortex state. Journal of Magnetism and Magnetic Materials. 2016;414:158-167.
5. Kashi MA, Ramazani A, Khayyatian A. The influence of the ac electrodeposition conditions on the magnetic properties and microstructure of Co nanowire arrays. J Phys D: Appl Phys. 2006;39(19):4130-4135.
6. Javed K, Zhang XM, Parajuli S, Ali SS, Ahmad N, Shah SA, et al. Magnetization behavior of NiMnGa alloy nanowires prepared by DC electrodeposition. Journal of Magnetism and Magnetic Materials. 2020;498:166232.
7. Najafi M, Soltanian S, Danyali H, Hallaj R, Salimi A, Elahi SM, et al. Preparation of cobalt nanowires in porous aluminum oxide: Study of the effect of barrier layer. Journal of Materials Research. 2012;27(18):2382-2390.
8. Koohbor M, Soltanian S, Najafi M, Servati P. Fabrication of CoZn alloy nanowire arrays: Significant improvement in magnetic properties by annealing process. Materials Chemistry and Physics. 2012;131(3):728-734.
9. Najafi M, Assari P, Rafati AA, Hamehvaisy M. Effect of the Electrodeposition Frequency, Wave Form, and Thermal Annealing on Magnetic Properties of $[Co_{0.975}Cr_{0.025}]_{0.99}Cu_{0.01}$ Nanowire Arrays. Journal of Superconductivity and Novel Magnetism. 2014;27(12):2821-2827.
10. Alonso J, Khurshid H, Sankar V, Nemati Z, Phan MH, Garayo E, et al. FeCo nanowires with enhanced heating powers and controllable dimensions for magnetic hyperthermia. Journal of Applied Physics. 2015;117(17):17D113.
11. Fu JL, Yan ZJ, Xu Y, Fan XL, Xue DS. Effects of annealing temperature on structure and magnetic properties of amorphous $Fe_{61}Co_{27}P_{12}$ nanowire arrays. Journal of Physics and Chemistry of Solids. 2007;68(12):2221-2226.
12. Wang RL, Tang SL, Shi YG, Fei XL, Nie B, Du YW. Effects of annealing on the structure and magnetic properties of $Fe_{27}Co_{23}Pb_{50}$ nanowire arrays. Journal of Applied Physics. 2008;103(7):07D507.
13. Gupta A, Ruwali K, Paul N, Duhaj P. Crystallization behavior of amorphous $(Fe_{100-x}Co_x)$85B15. Materials Science and Engineering: A. 2001;304-306:371-374.
14. Sedghi A, Zolfi F, Vali Aghaie S. Fabrication and Study of the Magnetic Properties of $(Fe_{30}Co_{70})_{100-x}Zn_x$ Nanowire Arrays. Acta Physica Polonica A. 2015;127(6):1706-1711.
15. Bran C, Ivanov YP, García J, del Real RP, Prida VM, Chubykalo-Fesenko O, et al. Tuning the magnetization reversal process of FeCoCu nanowire arrays by thermal annealing. Journal of Applied Physics. 2013;114(4):043908.
16. Ramazani A, Almasi-Kashi M, Golafshan E, Arefpour M. Magnetic behavior of as-deposited and annealed CoFe and CoFeCu nanowire arrays by ac-pulse electrodeposition. Journal of Crystal Growth. 2014;402:42-47.
17. Najafi M, Rafati AA, Fart MK, Zare A. Effect of the pH and electrodeposition frequency on magnetic properties of binary $Co_{1-x}Sn_x$ nanowire arrays. Journal of Materials Research. 2014;29(2):190-196.
18. Najafi M, Amjadi P, Alemipour Z. Fabrication and magnetic properties of ordered $Co_{100-x}Pb_x$ nanowire arrays electrodeposited in AAO templates: Effects of annealing temperature and frequency. Journal of Materials Research. 2017;32(6):1177-1183.
19. Guo J, Cui C, Yang W, Kang L, Zhang Y. Microstructures and magnetic properties of Tb-Fe-Co magnetic nanowire arrays prepared by electrochemical deposition. Superlattices and Microstructures. 2019;128:298-306.